is, the rating for long useful lifetime) versus calendar years (Fig. 8). The first 10-emitter arrays appeared in 1984 and were rated at 100 mW. Since that time, the reliable power level has approximately doubled every year, and 1-W devices are available today (*16*). It is likely that this rapid progression can be sustained for at least several more years.

The dashed line in Fig. 8 depicts "Moore's Law" for silicon integrated circuits. In the early 1970s, Gordon Moore, one of the founders of Intel Corporation, observed that the number of components that could be integrated onto a single silicon chip was doubling every 2 years. For comparison, the output power available from diode lasers is increasing at a rate twice as great. Thus substantial technological spin-off from these rapidly developing optical "integrated circuits" is certain to follow in the near future.

REFERENCES AND NOTES

1. G. L. Harnagel, D. R. Scifres, H. H. Kung, D. F. Welch, P. S. Cross, *Electron. Lett.* **22**, 605 (1986).
2. G. L. Harnagel, P. S. Cross, C. R. Lennon, M. DeVito, D. R. Scifres, *ibid.* **23**, 743 (1987).
3. G. L. Harnagel, P. S. Cross, C. R. Lennon, D. R. Scifres, in preparation.
4. D. R. Scifres, C. Lindstrom, R. D. Burnham, W. Streifer, T. L. Paoli, *Electron. Lett.* **19**, 169 (1983).
5. N. Holonyak, R. M. Kolbas, R. D. Dupuis, P. D. Dapkus, *IEEE J. Quantum Electron.* **QE-16**, 170 (1980).
6. R. D. Burnham, W. Streifer, D. R. Scifres, C. Lindstrom, T. L. Paoli, *Electron. Lett.* **18**, 1095 (1982).
7. K. Hamada *et al.*, *IEEE J. Quantum Electron.* **QE-21**, 623 (1985).
8. C. H. Henry, P. M. Petroff, R. A. Logan, F. R. Merritt, *J. Appl. Phys.* **50**, 3721 (1979).
9. D. F. Welch *et al.*, *Electron. Lett.* **22**, 464 (1986).
10. Model SDL-2430 from Spectra Diode Laboratories, San Jose, CA.
11. G. L. Harnagel *et al.*, *Appl. Phys. Lett.* **49**, 1418 (1986).
12. D. S. Hill *et al.*, in *Digest of the Topical Meeting on Semiconductor Lasers* (paper WB-8), Albuquerque, NM, 10 and 11 February 1987.
13. K. L. Chen and S. Wang, *Electron. Lett.* **22**, 644 (1986).
14. D. F. Welch, P. S. Cross, D. R. Scifres, W. Streifer, R. D. Burnham, *Appl. Phys. Lett.* **49**, 1632 (1986).
15. W. Streifer, P. S. Cross, D. F. Welch, D. R. Scifres, *ibid.*, p. 58.
16. Model SDL-2460 from Spectra Diode Laboratories, San Jose, CA.

17. We thank D. P. Worland, C. Lennon, and H. H. Kung for many useful technical discussions and the Defense Advanced Research Projects Agency and the Naval Ocean Systems Center for support of the two-dimensional array work.

Activated Oncogenes in B6C3F1 Mouse Liver Tumors: Implications for Risk Assessment

STEVEN H. REYNOLDS,* SHARI J. STOWERS, RACHEL M. PATTERSON, ROBERT R. MARONPOT, STUART A. AARONSON, MARSHALL W. ANDERSON

The validity of mouse liver tumor end points in assessing the potential hazards of chemical exposure to humans is a controversial but important issue, since liver neoplasia in mice is the most frequent tumor target tissue end point in 2-year carcinogenicity studies. The ability to distinguish between promotion of background tumors versus a genotoxic mechanism of tumor initiation by chemical treatment would aid in the interpretation of rodent carcinogenesis data. Activated oncogenes in chemically induced and spontaneously occurring mouse liver tumors were examined and compared as one approach to determine the mechanism by which chemical treatment caused an increased incidence of mouse liver tumors. Data suggest that furan and furfural caused an increased incidence in mouse liver tumors at least in part by induction of novel weakly activating point mutations in *ras* genes even though both chemicals did not induce mutations in *Salmonella* assays. In addition to *ras* oncogenes, two activated *raf* genes and four non-*ras* transforming genes were detected. The B6C3F1 mouse liver may thus provide a sensitive assay system to detect various classes of proto-oncogenes that are susceptible to activation by carcinogenic insult. As illustrated with mouse liver tumors, analysis of activated oncogenes in spontaneously occurring and chemically induced rodent tumors will provide information at a molecular level to aid in the use of rodent carcinogenesis data for risk assessment.

SEVERAL APPROACHES HAVE BEEN USED TO IDENTIFY ENVIronmental agents that pose significant carcinogenic hazards to humans. Chemicals in the environment are assessed on the basis of epidemiologic evidence from exposed human populations, when available, with supportive evidence derived from short-term tests that correlate with carcinogenicity. However, most chemicals are classified as potentially hazardous to humans on the basis of long-term carcinogenesis studies in rodents. Although animal experiments are designed so as to mimic the route of human exposure in the environment or workplace, the doses used in animals are usually higher than those to which humans are actually exposed. High doses of a chemical are utilized to enhance the sensitivity of the assay, since economic considerations limit the number of animals that can be used per study. The extrapolation of rodent carcinogenic data to human risk is complicated by the higher doses used in animals, and especially by the absence of information regarding the mechanisms of tumor induction.

Short-term tests have been utilized to evaluate the potential hazards of chemicals to humans. These tests have been popular because they can be performed quickly and inexpensively relative to long-term rodent carcinogenesis assays. Initially, many of the chemi-

S. H. Reynolds, S. J. Stowers, R. M. Patterson, M. W. Anderson, Laboratory of Biochemical Risk Analysis, National Institute of Environmental Health Sciences, Post Office Box 12233, Research Triangle Park, NC 27709. R. R. Maronpot, National Toxicology Program, National Institute of Environmental Health Sciences, Post Office Box 12233, Research Triangle Park, NC 27709. S. A. Aaronson, Laboratory of Cellular and Molecular Biology, National Institutes of Health, Bethesda, MD 20205.

*To whom reprint requests should be addressed.

Table 1. Transforming genes in chemically induced hepatocellular tumors of the B6C3F1 mouse. DNA transfection analysis was carried out by the calcium phosphate coprecipitation method as described (*10*). NIH/3T3 cells, plated 24 hours earlier at 2×10^5 cells per 10-cm dish in Dulbecco's modified Eagle's medium (DMEM) supplemented with 10% calf serum, were exposed for 22 hours to the DNA precipitate (20 μg per dish). Cultures were maintained with twice weekly changes of DMEM containing 5% calf serum. Focus formation was scored at 14 to 35 days.

DNA source	Frequency*	Transformation efficiency (foci per microgram of DNA)	
		Tumor DNA	Transfectant DNA, first cycle
Normal liver†	0/4	0.00	
Furan-induced tumor			
Hepatocellular adenoma	9/19	0.03–0.16	0.38–1.25
Hepatocellular carcinoma	4/10	0.01–0.06	0.63–1.25
Furfural-induced tumor			
Hepatocellular adenoma	2/3	0.03–0.05	0.81–1.88
Hepatocellular carcinoma	11/13	0.01–0.09	0.64–1.88

*Number positive/number tested. †Liver tissue of mice treated with furan or furfural in which no tumors were observed.

cals that tested positive in rodent carcinogenicity assays were also genotoxic in short-term tests. An agreement of 90% or greater was observed between carcinogenicity in rodents and mutagenicity in the *Salmonella* assay (*1*). Thus one common mechanism of action for rodent carcinogens was assumed to be the formation of promutagenic lesions in DNA. However, recent analysis of 73 chemicals tested in the National Toxicology Program (NTP) and National Cancer Institute (NCI) carcinogenesis studies showed a significant discordance between rodent carcinogenicity and genotoxicity in short-term tests (*2*). Of the 44 chemicals that tested positive for rodent carcinogenicity, 24 were negative for mutagenicity in the *Salmonella* assay. This lack of agreement between rodent carcinogenicity and mutagenicity in short-term tests further complicates risk analysis based on rodent carcinogenesis data.

Several explanations, in addition to cytotoxic effects, could account for the carcinogenicity of these chemicals in rodents and their lack of mutagenicity in short-term tests. In model systems for liver carcinogenesis, two of these compounds demonstrate tumor-promoting capabilities (*2*). Tumor promoters may exert their action independent of mutagenic effects by expanding the clonal outgrowth of cells that have previously undergone genetic damage. Another possibility is that the metabolic system required to activate a chemical to a carcinogen is not simulated in the short-term tests. The diversity of metabolic systems to activate chemicals and the potential to detect chemicals that interact at various stages of the multi-step process of neoplasia makes the animal a more sensitive system to detect potential carcinogens.

The tumor type or types that occur spontaneously or that are induced with a chemical are dependent on the species and strain of rodent employed in the carcinogenesis study. For purposes of risk analysis of rodent carcinogenesis data, we feel that a mechanism of tumor induction is much more important than the tumor type. We illustrate an approach to examine the mechanism of tumor induction in mouse liver tumors.

The B6C3F1 mouse has been used in NTP and NCI carcinogenesis studies since 1971. The interpretation of tumor responses in the liver of this strain continues to be the subject of active debate (*3*). Resolution of the scientific controversy as to the validity and usefulness of mouse liver tumor end points in assessing potential hazards to humans is of considerable importance since this tissue is the most frequent target tissue in NTP and NCI carcinogenesis studies. Of 278 compounds evaluated through June 1984, 141 (51%) were found to be carcinogenic and of these, 50% (70 out of 141) gave positive tumor responses in the mouse liver (*3*). The debate revolves around a possible connection between the high incidence of spontaneously occurring liver tumors and the high frequency of chemically induced liver tumors in this mouse strain. One view is that the relatively high doses of a chemical used in a typical study could promote the spontaneous liver lesions, by a cytotoxic mechanism, to a greater degree than observed in the control group. For example, 50% (12 out of 24) of the rodent carcinogens that were negative in the *Salmonella* assay gave tumor responses in the mouse liver (*2*). In contrast, the mouse liver may be a sensitive system to detect certain classes of chemicals that cause somatic mutations or have specific noncytotoxic promotional actions.

Increasing evidence suggests that conversion of proto-oncogenes to oncogenes by genetic alterations contributes to the neoplastic transformation of cells. These genetic alterations can range from point mutation to gross DNA rearrangements such as translocation and gene amplification (*4*). For example, members of the *ras* gene family, H-, K-, and N-*ras*, and the *neu* proto-oncogene can acquire transforming activity by a single point mutation in their coding sequence. Point mutations in the *ras* genes have been observed at codons 12, 13, and 61 in primary human and rodent tumors (*5, 6*). The activated *ras* genes, as well as *neu*, were detected by the NIH/3T3 transfection assay or by use of an in vivo selection assay in nude mice. These assays have also detected a number of other oncogenes in primary tumors or tumor cell lines (*7*). Investigations in several rodent models for chemical carcinogenesis imply that oncogenes are activated by carcinogen treatment and that this activation process is causally involved in tumor induction (*8, 9*).

Recently, we and others have detected oncogenes in 80% of spontaneously occurring hepatocellular carcinomas of the B6C3F1

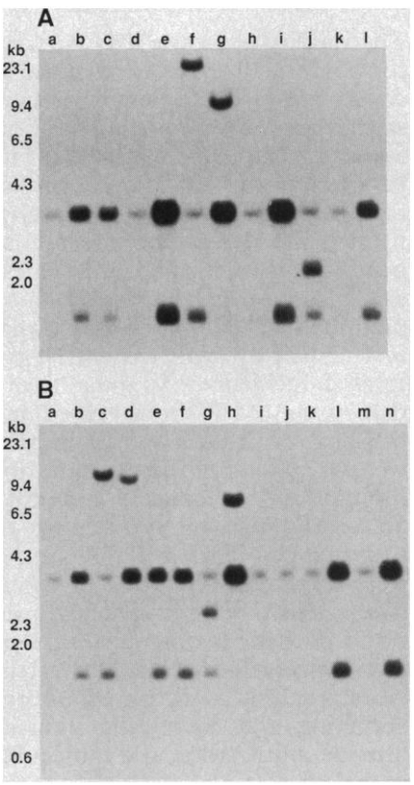

Fig. 1. Southern blot analysis of H-*ras* sequences in representative NIH/3T3 transformants induced by transfection of DNA from individual chemically induced mouse liver tumors. (**A**) Lanes: a, NIH/3T3 DNA; NIH/3T3 transformant DNAs derived from transfection with (b–i) furan-induced liver adenoma DNAs or with (j–l) furan-induced liver carcinoma DNAs. (**B**) Lanes: a, NIH/3T3 DNA; NIH/3T3 transformant DNAs derived from transfection with (b and c) furfural-induced liver adenoma DNAs or with (d–n) furfural-induced liver carcinoma DNAs. Normal and transfectant DNAs (20 μg of each) were digested with restriction endonuclease Bam HI, fractionated by electrophoresis through a 0.7% agarose gel and Southern blotted as described previously (*10*). The probe was a 0.73-kbp Sst I–Pst I fragment of the Harvey murine sarcoma virus *ras* gene (*32*). Numbers on the left are kilobases.

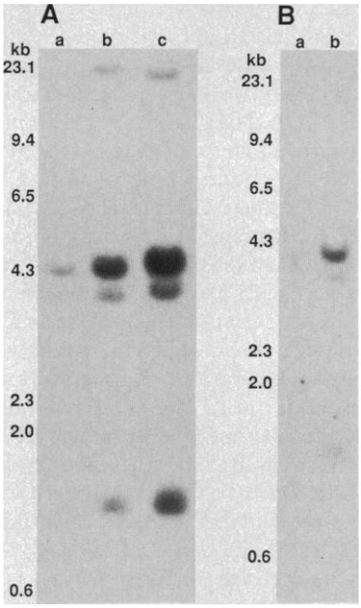

Fig. 2. Southern blot analysis of K-*ras* sequences in representative NIH/3T3 transformants derived from transfection of chemically induced liver tumor DNAs. (**A**) Lanes: a, NIH/3T3 DNA; b and c, NIH/3T3 transformants derived from transfection with furan-induced liver adenoma DNAs. (**B**) Lanes: a, NIH/3T3 DNA; b, NIH/3T3 transformant derived from transfection with furfural-induced liver carcinoma DNA. Normal and transfectant DNAs were digested with restriction endonuclease Hind III, separated by electrophoresis, and Southern blotted as described in Fig. 1. The probe was a 0.618-kbp Sst II–Hinc II fragment of the Kirsten murine sarcoma virus *ras* gene (*33*). (A) lanes b and c, and (B), lane b, correspond to the representative foci DNAs shown in Fig. 1A, lanes d and h, and Fig. 1B, lane k, respectively.

mouse and to a lesser degree (30%) in benign liver neoplasia (*10, 11*). We identified the majority of these oncogenes as activated c-H-*ras* genes and suggested that lesions had occurred in codon 61 on the basis of immunoprecipitation analysis of the transforming *ras* proteins (*10*). Although the mechanism of activation of the oncogenes detected in spontaneous mouse liver tumors is unknown, oncogene activation is probably one step in mouse liver tumor development. These findings suggest that one approach to determine the mechanism or mechanisms by which a chemical causes an increased incidence in rodent tumors is to compare oncogene activation in spontaneous and chemically induced tumors. For example, if the activated oncogenes detected in chemically induced tumors were different from those found in spontaneous tumors, then one could argue that the chemical itself activated the proto-oncogene by a genotoxic mechanism. Alternatively, the detection of similar activating lesions in oncogenes could imply that the chemical was increasing the background tumor incidence by a mechanism such as cytotoxicity or receptor-mediated promotion. The present study evaluates this approach by analysis of mouse liver tumors obtained from animals treated with furan or furfural, two compounds that test positive for tumor induction in the mouse liver in 2-year carcinogenicity studies (*12*) but that test negative for induction of mutations in *Salmonella* assays (*13*).

Detection of Transforming Genes in Chemically Induced Liver Tumors

Two sets of chemically induced B6C3F1 mouse liver tumors were examined for the presence of activated oncogenes by DNA transfection techniques. As shown in Table 1, transfection analysis indicated the presence of transforming genes in both benign and malignant hepatocellular tumors. DNA from 9 of 19 furan-induced hepatocellular adenomas and 4 of 10 furan-induced hepatocellular carcinomas scored positive for focus formation in the NIH/3T3 transfection assay. Similarly, DNA from 2 of 3 furfural-induced hepatocellular adenomas and 11 of 13 furfural-induced hepatocellular carcinomas scored positive by DNA transfection. The observed transforming efficiencies of the DNAs from chemically induced liver tumors (Table 1) were comparable to the transforming efficiencies seen with spontaneous liver tumor DNAs of the B6C3F1 mouse (*10, 11*). In each case the transforming gene was found to be stable upon serial transfer. The primary transfectant DNAs had an 8- to 80-fold increase in transfection efficiency as compared to the liver tumor DNAs (Table 1), which implies that amplification of the transforming gene had occurred in the primary transfectants, an event frequently observed during the transfection process. No foci were observed when NIH/3T3 cells were transfected with DNA isolated from the normal liver tissues of chemically treated B6C3F1 mice (Table 1).

The possibility that the tumors diagnosed as adenomas may contain focal areas of malignantly transformed cells in histologically unexamined areas cannot be excluded. However, the transforming efficiencies of the transfection-positive adenoma DNAs were comparable to those of the transfection-positive carcinoma DNAs (Table 1). This indicates that the transfection results for the positive adenomas cannot be attributed to the presence of a small minority of carcinoma cells within these adenomas.

Identification of Oncogenes in B6C3F1 Mouse Liver Tumors

Primary transfectant DNAs were initially analyzed by Southern blotting and hybridization with probes specific for H-, K-, and N-*ras*, since *ras* oncogenes are frequently detected by DNA transfection techniques. Hybridization of the primary transfectant DNAs with a mouse N-*ras*–specific probe (fourth exon) gave identical intensities and patterns of hybridization relative to normal NIH/3T3 DNA. However, with H-*ras* as a probe, DNAs from representative foci induced by 10 of 13 furan-induced liver tumor DNAs (for example, Fig. 1A, lanes b, c, e to g, i, j, and l; the data for two DNA transfectants from furan-induced liver tumors are not shown) exhibited a striking increase in hybridization intensity as compared to normal NIH/3T3 DNA (Fig. 1A, lane a). Similarly, DNAs from representative foci induced by 9 of 13 furfural-induced liver tumor DNAs (Fig. 1B, lanes b, c, d to h, l, and n) showed increased hybridization relative to NIH/3T3 DNA (Fig. 1B, lane a). Several

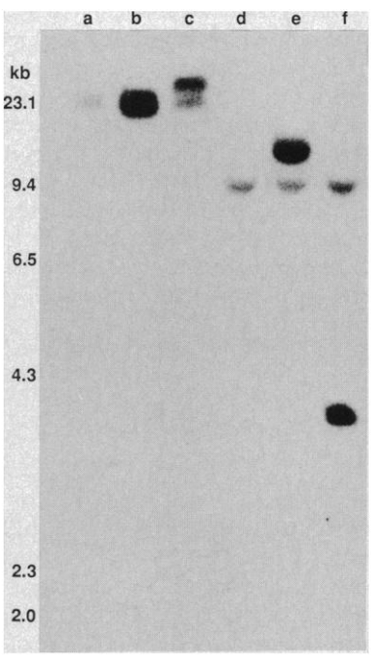

Fig. 3. Southern blot analysis of *raf* sequences in representative NIH/3T3 transformants derived from transfection of spontaneous or furan-induced liver tumor DNAs. Lanes: a and d, NIH/3T3 DNA; b and e, NIH/3T3 transformant DNA derived from transfection of spontaneous liver carcinoma DNA; c and f, NIH/3T3 transformant DNA derived from transfection of furan-induced liver carcinoma DNA. Normal and transfectant DNAs were digested with restriction endonucleases Hind III (lanes a to c) or Xba I (lanes d to f), separated by electrophoresis, and Southern blotted as described in Fig. 1. The probe was a 0.290-kbp Xho I–Sst I fragment of the 3611 murine sarcoma virus *raf* gene (*34*).

Table 2. Activated oncogenes detected in hepatocellular tumors of the B6C3F1 mouse. The sample size for the spontaneous liver tumors has been expanded since previously reported (*10*). Four additional hepatocellular carcinomas were examined by DNA transfection techniques, Southern blot, and oligonucleotide hybridization analysis. Each of these four additional hepatocellular carcinomas was found to contain an activated H-*ras* gene with a mutation at codon 61.

Treatment	Tumor type	Transfection frequency*	Activated oncogenes			
			H-*ras*	K-*ras*	*raf*	Unknown
Vehicle	Adenoma	3/10	3			
Vehicle	Carcinoma	14/17	12		1	1
Furan	Adenoma	9/19	7	2		
Furan	Carcinoma	4/10	3		1	
Furfural	Adenoma	2/3	2			
Furfural	Carcinoma	11/13	7	1		3

*Tumors positive/tumors tested.

transfectant DNAs (Fig. 1A, lanes f, g, and j; Fig. 1B, lanes c, d, g, and h) also demonstrated additional amplified H-*ras* DNA fragments of varying size. These findings suggest that these transfectants had incorporated tumor-derived alleles of the c-H-*ras* gene. Similarly, hybridization of the primary foci DNAs with a K-*ras*–specific probe suggests that 2 of 13 furan-induced liver tumor transfectant DNAs (Fig. 2A, lanes b and c) and 1 of 13 furfural-induced liver tumor transfectant DNAs (Fig. 2B, lane b) had incorporated tumor-derived alleles of the c-K-*ras* gene.

One of the furan-induced liver carcinoma DNAs, three of the furfural-induced liver carcinoma DNAs, and two spontaneous liver carcinoma DNAs (*10*) yielded foci that lacked evidence of amplified or rearranged *ras* genes. Representative foci DNAs induced by one of the spontaneous liver carcinoma DNAs (Fig. 3, lanes b and e) and the remaining furan-induced liver carcinoma DNA (Fig. 3, lanes c and f) showed amplified or rearranged hybridization signals to v-*raf* (or both) when compared to normal NIH/3T3 DNA (Fig. 3, lanes a and d). Two *raf*-containing foci were detected on separate tissue culture plates by transfection of the spontaneous liver tumor DNA, whereas only one *raf*-containing focus was detected by transfection of the furan-induced liver tumor DNA. *Raf* oncogenes have been shown to be artifactually activated by rearrangement during DNA transfection (*14*); therefore, it is possible that the single *raf*-containing focus observed by transfection of the furan-induced liver tumor DNA represents the results of in vitro activation. The three furfural-induced liver carcinoma DNAs and the other spontaneous liver carcinoma DNA, all of which contained non-*ras* oncogenes, each yielded two or more foci that were stable upon serial transfer. Cotransfection with a marker DNA indicated that the foci observed in NIH/3T3 cells had taken up exogenously added DNA. These results lead us to conclude that these genes were activated by somatic events within the tumor cells rather than as a result of the DNA transfection technique. Table 2 summarizes the activated oncogenes detected in the spontaneous and chemically induced mouse liver tumors.

Heterogeneity in Structural Alterations of Activated *ras* Proteins

A number of recent reports have shown that *ras* genes that have point mutations in their coding sequences frequently produce p21 proteins with altered electrophoretic mobilities. Slower or faster electrophoretic mobilities appear to accompany many of the activating lesions at codons 12 and 61, respectively (*15*). Therefore, the first-cycle liver tumor DNA transfectants derived from chemically induced tumors were analyzed for the presence of *ras* proteins with altered electrophoretic mobility.

Cells were labeled with [^{35}S]methionine and analyzed for p21 expression by immunoprecipitation with monoclonal antibody Y13-259 (*16*). NIH/3T3 cells transformed by the c-H-*ras* T24 oncogene (activated at codon 12) produced a p21 that migrated as a slow-moving species (Fig. 4, A and B, lanes b) relative to mouse endogenous p21 bands (Fig. 4, A and B, lanes a). In contrast, NIH/3T3 cells transformed by a c-H-*ras* Hs242 gene activated at codon 61 produced a p21 that migrated as a fast-moving species (Fig. 4, A and B, lanes c). The DNA transfectants that contained an activated c-H-*ras* gene produced p21 proteins that migrated as either a slow-moving species (Fig. 4A, lanes g, i, k, l, and n; Fig. 4B, lanes e, n, and p) or a fast-moving species (Fig. 4A, lanes d, e, and h; Fig. 4B, lanes d, f to j). The two furan-induced liver tumor DNA transfectants that contained activated c-K-*ras* oncogenes gave p21 proteins with a much slower than normal electrophoretic mobility (Fig. 4A, lanes f and j). Conversely, the furfural-induced liver tumor DNA transfectant that contained an activated c-K-*ras* oncogene gave a p21 protein with only a slightly slower than normal electrophoretic mobility (Fig. 4B, lane m). As expected, the furan-induced liver tumor DNA transfectant containing an activated *raf* oncogene (Fig. 4A, lane m) and the three furfural-induced liver tumor DNA transfectants containing non-*ras* oncogenes (Fig. 4B, lanes k, l, and o) yielded only p21 proteins with a normal electrophoretic mobility. The slower than normal electrophoretic mobility of some of the mutated c-H-*ras* proteins observed in the furan- and furfural-induced liver tumor DNA transfectants is in contrast with the mobilities of the mutated c-H-*ras* proteins observed in the spontaneous liver tumor DNA transfectants, where only faster than normal mobilities were observed (*10*).

Oligonucleotide Analysis of Activating Mutations in *ras* Oncogenes

Synthetic 19-mer oligonucleotide probes were used to analyze the transfected *ras* oncogenes detected in the spontaneous and chemically induced hepatocellular tumors. Oligonucleotide analysis allows detection of mutations in fixed positions based on the fact that a

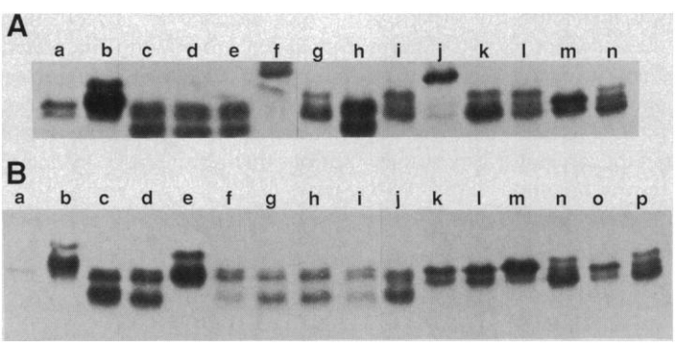

Fig. 4. Heterogeneity in the electrophoretic mobilities of activated p21 *ras* proteins from NIH/3T3 transformants induced by DNAs of chemically induced liver tumors. (**A**) Lanes: a, NIH/3T3 cells; b, NIH/3T3 cells transformed by T24 oncogene; c, NIH/3T3 cells transformed by Hs242 oncogene; NIH/3T3 transformants of (d to k) furan-induced liver adenoma DNAs or (l to n) furan-induced liver carcinoma DNAs. (**B**) Lanes: a, NIH/3T3 cells; b, NIH/3T3 cells transformed by T24 oncogene; c, NIH/3T3 cells transformed by Hs242 oncogene; NIH/3T3 transformants of (d and e) furfural-induced liver adenoma DNAs or (f to p) furfural-induced liver carcinoma DNAs. First-cycle NIH/3T3 transformants were labeled with [^{35}S]methionine, lysates were immunoprecipitated with p21 monoclonal antibody Y13-259, and immunoprecipitates were analyzed by SDS–14% polyacrylamide gel electrophoresis as described (*10*).

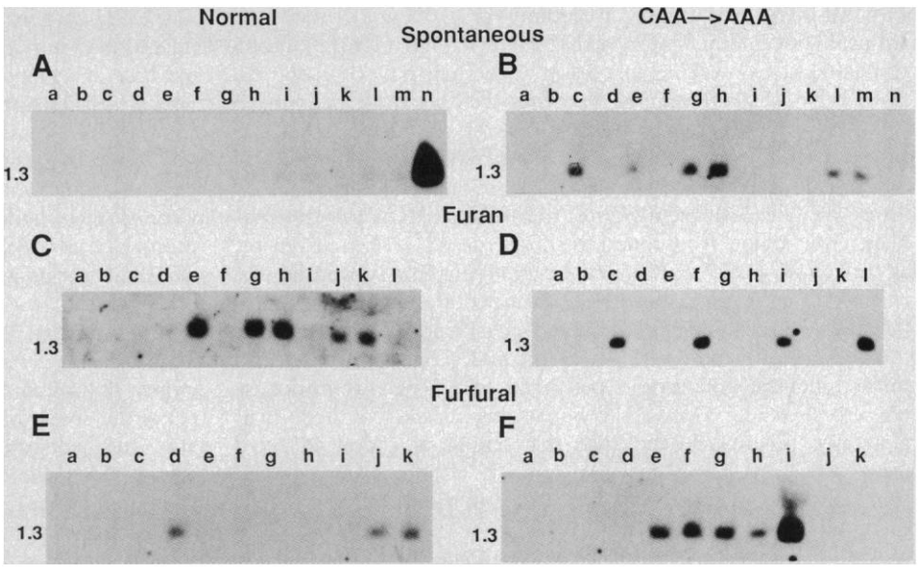

Fig. 5. Hybridization of synthetic oligomer probes centered on codon 61 of the rat H-*ras* gene to genomic DNA of normal tissue and NIH/3T3 transfectants of spontaneous and chemically induced liver tumor DNAs. (**A** and **B**) Lanes: a, NIH/3T3 DNA; b, normal mouse liver DNA; NIH/3T3 transformants derived from transfection with (c to e) spontaneous liver adenoma DNAs or (f to m) spontaneous liver carcinoma DNAs; n, S80-1-1 cell line DNA. (**C** and **D**) Lanes: a, NIH/3T3 DNA; b, normal mouse liver DNA; NIH/3T3 transformants derived from transfection with (c to i) furan-induced liver adenoma DNAs or (j to l) furan-induced liver carcinoma DNAs. (**E** and **F**) Lanes: a, NIH/3T3 DNA; b, normal mouse liver DNA; NIH/3T3 transformants derived from transfection with (c and d) furfural-induced liver adenoma DNAs or (e to k) furfural-induced liver carcinoma DNAs. Samples (20 μg) of each DNA were digested with restriction endonuclease Pvu II and separated by electrophoresis in a 0.7% agarose gel. The DNA was denatured in situ in 0.5*M* NaOH, 0.8*M* NaCl (1 hour at room temperature) and neutralized in 1*M* tris HCl (*p*H 7.5), 1.5*M* NaCl (1 hour at room temperature). Gels were then dried and prehybridized in 6× standard saline citrate (SSC), 10× Denhardt's solution, 200 μg/ml denatured and sheared herring sperm DNA, 0.1% SDS and 20 m*M* tris HCl (*p*H 7.6). Gels were hybridized in 50% formamide, 5× SSC, 5× Denhardt's solution, 100 μg/ml denatured and sonicated herring sperm DNA, 0.1% SDS and 20 m*M* tris HCl (*p*H 7.6) at 42°C. Probes were labeled by the primer extension method as described by Bos *et al.* (*6*). Gels A, C, and E were hybridized to a 19-mer probe centered on the second base of codon 61 of the rat H-*ras* gene (5′-CAGCAGGT*CAA*GAAGAGTA-3′). Gels B, D, and F were hybridized to a 19-mer probe centered on the second base of codon 61 of the rat c-H-*ras* gene containing a CG→AT transversion at the first base of codon 61 (5′-CAGCAGGT*AAA*GAAGAGTA-3′). Melting point temperature (T_m) for a perfectly matched hybrid was calculated from the formula T_m = 4°C (number of GC pairs) + 2°C (number of AT pairs) for 19-mer oligonucleotide probes. Hybridized gels were washed first in 2× SSC for 30 minutes at 10°C below T_m (poured onto the gel and then shaken at room temperature) and then in 2× SSC for 10 minutes at T_m (poured onto the gel and then shaken at room temperature).

perfectly matched DNA hybrid has a higher thermal stability than a hybrid with a mismatched base pair. Selective wash procedures result in the removal of mismatched hybrids, whereas a completely matched hybrid remains stable (*17*). This technique has been used by several investigators to identify point mutations in activated *ras* genes (*6, 8, 9, 18*). A summary of the activating mutations detected in the transforming H-*ras* genes is presented in Table 3, and the following is a description of the analysis by which we characterized the mutations.

We first analyzed the transfectant DNAs that contained activated H-*ras* genes for mutations at codons 12 and 61. Pvu II–digested DNAs from the spontaneous and chemically induced liver tumor DNA transfectants were hybridized to a 19-mer probe corresponding to the normal sequence of the rat c-H-*ras* gene (*19*) centered on codon 61 (H61-N) and washed under conditions in which only a perfectly matched hybrid was stable (Fig. 5, A, C, and E). All of the transfectant DNAs from spontaneous liver tumors (Fig. 5A, lanes c to m) gave hybridization signals that were comparable to those seen with NIH/3T3 or normal mouse liver DNA (Fig. 5A, lanes a and b, respectively). DNA from the NIH/3T3 cell line S80-1-1, which contains amplified copies of the normal rat c-H-*ras* sequence, gave an intense hybridization signal with the H61-N probe (Fig. 5A, lane n). Similarly, five of ten transfectant DNAs from furan-induced liver tumors (Fig. 5C, lanes c, d, f, i, and l) and six of nine transfectant DNAs from furfural-induced liver tumors (Fig. 5E, lanes c and e to i) gave hybridization signals that were comparable to those seen with NIH/3T3 or normal mouse liver DNA (Figs. 5, C and E, lanes a and b, respectively). Collectively, these results indicate the presence of a mutation in or adjacent to codon 61 in the transfected H-*ras* genes which failed to hybridize to the H61-N probe.

The same gels shown in Fig. 5, A, C, and E, were subsequently hybridized to 19-mer probes containing all possible activating mutations at codon 61 of the rat c-H-*ras* gene. Six of 11 transfectant DNAs from spontaneous liver tumors (Fig. 5B, lanes c, e, g, h, l, and m), four of ten transfectant DNAs from furan-induced liver tumors (Fig. 5D, lanes c, f, i, and l), and five of nine transfectant

Table 3. Pattern of mutations in H-*ras* genes in liver tumors of the B6C3F1 mouse.

Treatment and tumor type	Activated H-*ras*	Codon 61				Codon 13			Codon 117		
		Normal	Mutations			Normal	Mutations		Normal	Mutations	
		CAA→	AAA	CTA	CGA	GGC→	GTC	CGC	AAG→	AAC	AAT
Vehicle											
Adenoma	3		2	1	0						
Carcinoma	12		7	2	3						
Furan											
Adenoma	7		3	0	1					2	1
Carcinoma	3		1	0	0					0	1
Furfural											
Adenoma	2		0	0	1		0	1		0	0
Carcinoma	7		5	0	0		1	0		0	1

DNAs from furfural-induced liver tumors (Fig. 5E, lanes e to i) gave strong hybridization signals with a 19-mer oligonucleotide probe containing a CG →AT transversion at the first base of codon 61 (H61-A1). Thus, these c-H-*ras* genes were each activated by a CG →AT transversion at the first base of codon 61 leading to substitution of lysine for the normal glutamine. The amplified c-H-*ras* normal rat sequence showed no cross-hybridization to the H61-A1 probe (Fig. 5B, lane n). Three transfectant DNAs from spontaneous liver tumors were found to contain an AT→TA transversion at the second position of codon 61, resulting in a substitution of leucine for glutamine. Further oligonucleotide analysis indicated that the two remaining transfectant DNAs from spontaneous liver tumors and one each of the transfectant DNAs from furan- and furfural-induced liver tumors contained an AT→GC transition at the second base of codon 61, giving arginine instead of the normal glutamine. These data indicated that lesions at codon 61 were responsible for c-H-*ras* gene activation in all of the transfectants from spontaneous liver tumors and some of the transfectants from chemically induced liver tumors.

The furan- and furfural-induced liver tumor transfectant DNAs that had normal c-H-*ras* gene sequences at codon 61 were subsequently hybridized to 19-mer oligonucleotide probes centered on either codon 12 (H12-N) or codon 13 (H13-N) of the mouse c-H-*ras* gene sequence. Two transfectant DNAs from furfural-induced liver tumors failed to hybridize to either the H13-N probe (Fig. 6A, lanes b and d) or the H12-N probe. Screening of these transfectant DNAs with 19-mer oligonucleotide probes that correspond to all possible activating mutations at codon 12 and codon 13 of the mouse c-H-*ras* gene identified one transfectant DNA from furfural-induced liver tumors as containing a GC → CG transversion at the first base of codon 13 (GGC → CGC) (Fig. 6B, lane b) and one transfectant DNA from furfural-induced liver tumors as containing a GC →TA transversion at the second base of codon 13 (GGC → GTC) (Fig. 6C, lane d). The amplified c-H-*ras* gene sequence from normal rat showed no cross-hybridization to either of the 19-mer oligonucleotide probes with mutations at the first or second base of codon 13 (Fig. 6, B and C, lane a, respectively). The hybridization signal of the transfected c-H-*ras* gene in Fig. 6A, lane h, is relatively weak and is rearranged so that it appears near the bottom of the gel.

In vitro mutagenesis experiments have recently shown that mutations in the codon 116–119 region of the H-*ras* gene significantly reduce the ability of the H-*ras* p21 protein to bind and hydrolyze guanosine triphosphate (GTP) and that some mutations in this region are capable of activating the transforming potential of an otherwise normal H-*ras* gene (*20, 21*). The results of hybridization of a 19-mer oligonucleotide probe, H118-N, centered on codon 118 of the normal mouse c-H-*ras* gene sequence, to the undefined activated c-H-*ras* genes is shown in Fig. 7A. Five of the six H-*ras* transfectant DNAs (Fig. 7A, lanes d, f, g, h, and j) gave hybridization signals comparable to that seen with NIH/3T3 DNA (lane a) whereas stronger hybridization signals were observed with the amplified normal, rat c-H-*ras* gene (lane b), two H-*ras* transfectants previously defined as having codon 13 mutations (lanes c and e), an H-*ras* transfectant DNA previously defined as having a codon 61 mutation (lane k), and one of the H-*ras* transfectant DNAs (lane i). The hybridization signals in lanes c and i are rearranged and appear near the top and bottom of Fig. 7A, respectively. Further oligonucleotide probe analysis of the transfected H-*ras* genes that did not hybridize to the H118-N probe (Fig. 7, lanes d, f, g, h, and j) allowed us to localize the mutations in these H-*ras* genes to codon 117. Hybridization of the gel shown in Fig. 7A with 19-mer oligonucleotide probes that corresponded to all possible activating mutations at codon 117 identified two transfectant DNAs from

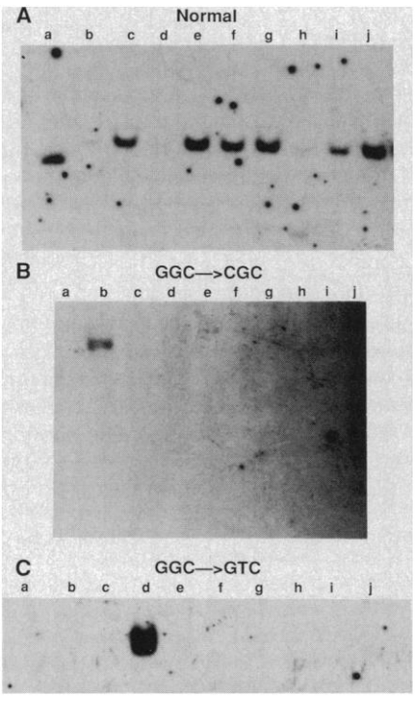

Fig. 6. Hybridization of synthetic oligomer probes centered on codon 13 of the mouse H-*ras* gene to genomic DNA of normal tissue and NIH/3T3 transfectants of chemically induced liver tumor DNAs. (**A**, **B**, and **C**) Lanes: a, S80-1-1 cell line DNA; NIH/3T3 transformants derived from transfection with (b) furfural-induced liver adenoma DNA or with (c and d) furfural-induced liver carcinoma DNAs; NIH/3T3 transformants derived from transfection with (e to g) furan-induced liver adenoma DNAs or with (h and i) furan-induced liver carcinoma DNAs; j, NIH/3T3 transformant containing a mouse H-*ras* gene with a mutation at codon 61 (CAA →AAA). DNAs were digested with restriction endonucleases Hind III (S80-1-1) or Bam HI (NIH/3T3 transformants), separated by electrophoresis, and processed as described in Fig. 5. Probes were end labeled with polynucleotide kinase as described by Zarbl *et al.* (*9*). Gel A was hybridized to a 19-mer probe centered on the middle base of codon 13 of the mouse H-*ras* gene (5′-GCGCTGGA*GGC*GTGGGAAA-3′). Gels B and C, respectively, were hybridized to 19-mer probes centered on the second base of codon 13, of the mouse H-*ras* gene with either a GC → CG transversion at the first base of codon 13 (5′-GCGCTGGA*CGC*GTGGGAAA-3′) or a GC → TA transversion at the second base of codon 13 (5′-GCGCTGGA*GTC*GTGGGAAA-3′), respectively. Gels were hybridized and washed as described in Fig. 5.

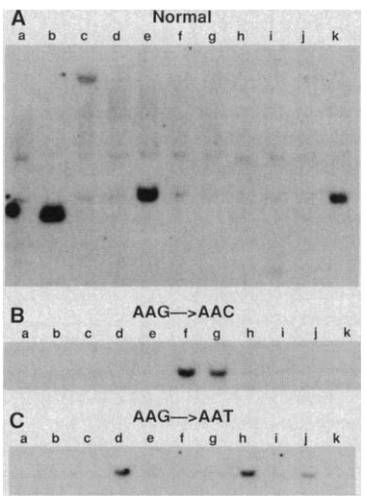

Fig. 7. Hybridization of synthetic oligomer probes centered on codon 117 or codon 118 of the mouse H-*ras* gene to genomic DNA of normal tissue and NIH/3T3 transfectants of chemically induced liver tumor DNAs. (**A**, **B**, and **C**) Lanes: a, NIH/3T3 DNA; b, S80-1-1 cell line DNA; NIH/3T3 transformants derived from transfection with (c) furfural-induced liver adenoma DNA or with (d and e) furfural-induced liver carcinoma DNAs; NIH/3T3 transformants derived from transfection with (f to h) furan-induced liver adenoma DNAs or with (i and j) furan-induced liver carcinoma DNAs; k, NIH/3T3 transformant containing a mouse H-*ras* gene with a mutation at codon 61 (CAA → AAA). DNAs were digested, separated by electrophoresis, hybridized, and washed as described in Fig. 5. Probes were end labeled as described in Fig. 6. Gel A was hybridized to a 19-mer probe centered on the second base of codon 118 of the mouse H-*ras* gene (5′-GCAACAAG*TGT*GACCTGGC-3′). Gels B and C, respectively, were hybridized to 19-mer probes centered on the second base of codon 117 of the mouse H-*ras* gene with either a GC → CG transversion at the third base of codon 117 (5′-TGGGCAAC*AAC*TGTGACCT-3′) or a GC → TA transversion at the third base of codon 117 (5′-TGGGCAAC*AAT*TGTGACCT-3′), respectively.

furan-induced liver tumors as containing GC → CG transversions at the third base of codon 117 (AAG → AAC) (Fig. 7B, lanes f and g). In addition, one transfectant DNA from furfural-induced liver tumors (Fig. 7C, lane d) and two transfectant DNAs from furan-induced liver tumors (Fig. 7C, lanes h and j) contained GC →TA transversions at the third base of codon 117 (AAG → AAT). The novel activating lesions at codon 13 and codon 117 of the H-*ras* gene reported here were also found to be present in the tumor DNAs from which they were derived. This indicates that these mutations resulted from somatic events that occurred within the tumor DNAs.

The activated K-*ras* gene derived from transfection with a furfural-induced liver tumor DNA was found to be activated by a mutation within or adjacent to codon 12 as determined by oligonucleotide probe analysis. Conversely, the activated K-*ras* genes derived from transfection with furan-induced liver tumor DNAs do not have mutations within or adjacent to codons 12, 13, 59–63, or 116–119. Furthermore, the activated H-*ras* gene shown in Fig. 7A, lane i, derived from transfection of a furan-induced liver tumor DNA, did not have mutations within or adjacent to codons 12, 13, 59–63, 83, 116–119, or 144. These regions of the *ras* gene family have been associated with various biochemical properties such as GTP binding and hydrolysis or GTP–guanosine diphosphate (GDP) exchange rates (*21–25*). The mechanism of activation of these H-*ras* and K-*ras* genes remains to be defined, but the altered mobilities of their protein products (Fig. 4) would be consistent with point mutations within their coding sequences.

Oncogene Activation in B6C3F1 Mouse Liver Tumors

A high frequency of activated oncogenes was detected in the spontaneous (*10, 11*) and chemically induced [(*18*), Table 1] hepatocellular tumors of the B6C3F1 mouse. Both *ras* and non-*ras* oncogenes were detected in these tumors (Table 2), similar to the results obtained by DNA transfection analysis of aflatoxin B_1–induced rat liver tumors (*26*). Ochiya *et al.* have also detected a non-*ras* oncogene in human hepatocellular carcinomas (*27*). The relation between the non-*ras* oncogenes derived from the rodent and human liver tumors is unclear at present.

A broad spectrum of activating point mutations in the H-*ras* gene were observed (Table 3), including mutations at codon 13 and codon 117, two codons that had not previously been shown to be activated in tumor DNAs. Activating mutations at codon 13 of the H-*ras* gene have been observed only in an in vitro mutagenesis assay with a cloned c-H-*ras* gene (*28*), whereas activating mutations at codon 117 of H-*ras* have not been observed either in vitro or in vivo. The foci induced by the codon 13 or codon 117 H-*ras* mutants were slower to appear and less morphologically transformed than are foci induced by the codon 12–activated T24 H-*ras* oncogene or the codon 61 H-*ras* mutants detected in the spontaneous liver tumors. A similar observation has been reported for codon 13–activated N-*ras* (*6*) and H-*ras* genes (*28*). The weaker morphological transformation of NIH/3T3 or Rat 1 cells by mutations in codon 13 (*28*) and the codon 116–119 (*21*) region of H-*ras* could in part account for the fact that these mutations have not been observed previously in human or animal tumor DNAs when assayed by the NIH/3T3 focus assay.

A recent study also suggests that the liver of the B6C3F1 mouse might be a sensitive model for the detection of activated oncogenes. Drinkwater and Ginsler found that at least two genetic loci control sensitivity to liver tumor induction in one of the B6C3F1 parental strains, the C3H/HeJ mouse (*29*). One locus, designated *Hcs*, may be responsible for 85% of the increased liver tumor susceptibility of the C3H/HeJ mouse (*29*). Furthermore, their data indicate that the *Hcs* gene primarily affects the promotion stage of liver tumor induction in the C3H/HeJ mouse (*29*). Therefore, weakly activating mutations in oncogenes, codon 13 or codon 117 in H-*ras*, may be effectively promoted and phenotypically expressed in the liver of the B6C3F1 mouse. The liver of the B6C3F1 mouse may thus be useful in the detection of various classes of proto-oncogenes that are susceptible to mutational activation and as a system that will allow phenotypic expression of weakly activating mutations in oncogenes.

Point mutations at codons 12 or 61 greatly reduce the intrinsic guanosine triphosphatase (GTPase) activity of H-*ras* proteins (*23, 24*) without affecting their guanine nucleotide–binding properties (*24, 25*), whereas activating point mutations in the codon 116–119 region can significantly reduce both the binding and hydrolysis of GTP (*21*). Several studies have indicated that there is no quantitative correlation between reduction in GTPase activity and transforming potential of activated H-*ras* genes (*24, 30*). The codon 13 and codon 117 mutants of H-*ras* could be useful in determining whether structural mutations result in allosteric changes that alter the affinity of regulatory or effector molecules for mutated *ras* proteins or whether structural modifications differentially alter a biochemical parameter such as the GTP-GDP exchange rate (*21, 31*) resulting in constitutively activated *ras* proteins. Furthermore, the H-*ras* and K-*ras* genes, that were activated by undefined mechanisms could potentially be useful in defining new domains within these genes that can be involved in the activation of *ras* proteins.

Interpretation of Mouse Liver Carcinogenic Data

The regulation of human occupational or environmental exposure to a chemical, based on long-term carcinogenesis studies in rodents, should take into account whether the chemical in question is mutagenic, cytotoxic, or has a receptor-mediated mechanism of promotion. Investigation of the pattern of oncogene activation in spontaneous and chemically induced mouse liver tumors allows an analysis of the mechanism of tumor formation at a molecular level. This type of analysis will be particularly useful for compounds such as furan and furfural, which do not induce mutations in short-term bacterial mutagenicity assays but test positive for liver tumor induction in the mouse on long-term rodent studies. The spectrum of activating mutations in the H-*ras* gene and the pattern of *ras* gene activation observed in the chemically induced liver tumors differ significantly from those observed in the liver tumors of untreated animals. All of the activated *ras* genes detected in the spontaneous liver tumors were H-*ras* with activating point mutations at codon 61. In contrast, 60% of the *ras* oncogenes detected in furan-induced liver tumors and 40% of the *ras* oncogenes detected in furfural-induced liver tumors were either activated K-*ras* genes or H-*ras* genes with mutations at positions other than codon 61 (Tables 2 and 3). These novel mutations in *ras* genes could have resulted from direct genotoxic effects of furan and furfural. An alternate mechanism is that these mutations were induced by an indirect secondary genotoxic pathway resulting from a cytotoxic event. However, the absence of cytotoxic lesions in the liver, based on histopathological examination after 90 days of administration of the chemicals at the carcinogenic dose, argues in favor of direct genotoxic mechanisms. Studies on the mutagenicity of furan and furfural in mammalian cells are in progress.

If mutations were observed only at codon 61 of the H-*ras* gene in chemically induced liver tumors, it is still possible that the mutations were due to DNA lesions induced by the chemical. For instance,

Wiseman *et al.* detected codon 61–activated H-*ras* genes in 24 of 25 mouse liver tumors that were induced by potent genotoxic carcinogens administered as a single dose to 12-day-old B6C3F1 mice (*18*). Therefore, in instances where the pattern of *ras* gene activation in chemically induced liver tumors closely parallels that observed in spontaneous liver tumors, it will be necessary to evaluate other parameters such as DNA adduct formation, cytotoxicity, or possible receptor binding.

The chemicals that are tested in long-term rodent carcinogenesis assays are often selected on the basis of their high occupational or environmental exposure. The results of this study provide a basis for the systematic analysis of activated oncogenes in spontaneously occurring and chemically induced tumors derived from long-term carcinogenesis studies in rodents. This approach may be particularly helpful in elucidating the mechanism of tumor induction by chemicals that test negative in short-term mutagenicity assays. Information at a molecular level will make the results from rodent carcinogenesis studies more relevant to the assessment of human risk.

REFERENCES AND NOTES

1. J. McCann, E. Choi, E. Yamasaki, B. N. Ames, *Proc. Natl. Acad. Sci. U.S.A.* **72**, 5135 (1975); I. F. H. Purchase *et al.*, *Nature (London)* **264**, 624 (1976).
2. R. W. Tennant *et al.*, *Science* **236**, 933 (1987).
3. R. R. Maronpot *et al.*, *Arch. Toxicol.*, in press.
4. M. J. Bishop, *Annu. Rev. Biochem.* **52**, 301 (1983); R. A. Weinberg, *Science* **230**, 770 (1985).
5. E. P. Reddy, R. K. Reynolds, E. Santos, M. Barbacid, *Nature (London)* **300**, 149 (1982); Y. Yuasa *et al.*, *ibid.* **303**, 775 (1983).
6. J. L. Bos *et al.*, *ibid.* **315**, 726 (1985).
7. C. S. Cooper *et al.*, *Cancer Res.* **44**, 1 (1984); C. Shih, L. C. Padhy, M. Murray, R. A. Weinberg, *Nature (London)* **290**, 261 (1981); R. A. Padua, N. Barrass, G. A. Currie, *ibid.* **311**, 671 (1984); A. Eva and S. A. Aaronson, *ibid.* **316**, 273 (1985); O. Fasano, D. Birnbaum, L. Edlund, J. Fogh, M. Wigler, *Mol. Cell. Biol.* **4**, 1695 (1984).
8. A. Balmain, M. Ramsden, G. T. Bowden, J. Smith, *Nature (London)* **307**, 658 (1984); D. Bizub, A. W. Wood, A. M. Skalka, *Proc. Natl. Acad. Sci. U.S.A.* **83**, 6048 (1986); I. Guerrero, A. Villasante, V. Corces, A. Pellicer, *Science* **225**, 1159 (1984).
9. H. Zarbl, S. Sukumar, A. V. Arthur, D. Martin-Zanca, M. Barbacid, *Nature (London)* **315**, 382 (1985).
10. S. H. Reynolds, S. J. Stowers, R. R. Maronpot, M. W. Anderson, S. A. Aaronson, *Proc. Natl. Acad. Sci. U.S.A.* **83**, 33 (1986).
11. T. R. Fox and P. G. Watanabe, *Science* **228**, 596 (1985).
12. Furan and furfural were tested for carcinogenicity in male and female B6C3F1 mice by the National Toxicology Program (NTP). Although both chemicals induced a two- to tenfold increase in benign and malignant liver neoplasia, official announcement of the results must await data audits of the studies and public peer reviews by the Technical Reports Review Subcommittee of the NTP Board of Scientific Counselors.
13. K. Mortelmans *et al.*, *Environ. Mutagen.* **8** (suppl. 7), 1 (1986).
14. F. Ishikawa, F. Takaku, K. Hayashi, M. Nagao, T. Sugimura, *Mol. Cell. Biol.* 7, 1226 (1987); V. P. Stanton and G. M. Cooper, *ibid.*, p. 1171.
15. S. K. Srivastava, Y. Yuasa, S. H. Reynolds, S. A. Aaronson, *Proc. Natl. Acad. Sci. U.S.A.* **82**, 38 (1985).
16. M. E. Furth, L. J. Davis, B. Fleurdelys, E. M. Scolnick, *J. Virol.* **43**, 294 (1982).
17. B. J. Conner *et al.*, *Proc. Natl. Acad. Sci. U.S.A.* **80**, 278 (1983).
18. R. W. Wiseman, S. J. Stowers, E. C. Miller, M. W. Anderson, J. A. Miller, *ibid.* **83**, 5825 (1986).
19. E. P. Reddy, D. Lipman, P. R. Andersen, S. R. Tronick, S. A. Aaronson, *J. Virol.* **53**, 984 (1985); M. Ruta *et al.*, *Mol. Cell. Biol.* **6**, 1706 (1986); R. Dhar *et al.*, *Science* **217**, 934 (1982).
20. D. J. Clanton, S. Hattori, T. Y. Shih, *Proc. Natl. Acad. Sci. U.S.A* **83**, 5076 (1986).
21. M. Walter, S. G. Clark, A. D. Levinson, *Science* **233**, 649 (1986).
22. L. A. Feig, B. Pan, T. M. Roberts, G. M. Cooper, *Proc. Natl. Acad. Sci. U.S.A.* **83**, 4607 (1986).
23. J. P. McGrath, D. J. Capon, D. V. Goeddel, A. D. Levinson, *Nature (London)* **310**, 644 (1984); R. W. Sweet *et al.*, *ibid.* **311**, 273 (1984); J. B. Gibbs, I. S. Sigal, M. Poe, E. M. Scolnick, *Proc. Natl. Acad. Sci. U.S.A.* **81**, 5704 (1984).
24. C. J. Der, T. Finkel, G. M. Cooper, *Cell* **44**, 167 (1986).
25. T. Finkel, C. J. Der, G. M. Cooper, *ibid.* **37**, 151 (1984).
26. G. McMahon, L. Hanson, J. Lee, G. N. Wogan, *Proc. Natl. Acad. Sci. U.S.A.* **83**, 9418 (1986).
27. T. Ochiya, A. Fujiyama, S. Fukushige, I. Hatada, K. Matsubara, *ibid.*, p. 4993.
28. O. Fasano *et al.*, *ibid.* **81**, 4008 (1984).
29. N. R. Drinkwater and J. J. Ginsler, *Carcinogenesis* 7, 1701 (1986).
30. J. C. Lacal, S. K. Srivastava, P. S. Anderson, S. A. Aaronson, *Cell* **44**, 609 (1986).
31. J. C. Lacal and S. A. Aaronson, *Mol. Cell. Biol.* **6**, 4214 (1986).
32. R. W. Ellis *et al.*, *Nature (London)* **292**, 506 (1981).
33. R. W. Ellis *et al.*, *Mol. Cell. Biol.* **2**, 1339 (1982).
34. T. Bonner *et al.*, *Science* **223**, 71 (1984).

35. We thank A. Pellicer and M. Barbacid for the gifts of the mouse fourth exon N-*ras* probe and the S80-1-1 cell line, respectively.